

# Ambient- and low-temperature synchrotron x-ray diffraction study of $\text{BaFe}_2\text{As}_2$ and $\text{CaFe}_2\text{As}_2$ at high pressures up to 56 GPa

R. Mittal,<sup>1</sup> S. K. Mishra,<sup>1</sup> S. L. Chaplot,<sup>1</sup> S. V. Ovsyannikov,<sup>2</sup> E. Greenberg,<sup>2,3</sup> D. M. Trots,<sup>2</sup> L. Dubrovinsky,<sup>2</sup> Y. Su,<sup>4</sup> Th. Brueckel,<sup>4,5</sup> S. Matsuishi,<sup>6</sup> H. Hosono,<sup>6</sup> and G. Garbarino<sup>7</sup>

<sup>1</sup>*Solid State Physics Division, Bhabha Atomic Research Centre, Trombay, Mumbai 400 085, India*

<sup>2</sup>*Bayerisches Geoinstitut, University Bayreuth, Universitätsstrasse 30, D-95440 Bayreuth, Germany*

<sup>3</sup>*School of Physics and Astronomy, Tel-Aviv University, Israel*

<sup>4</sup>*Jülich Centre for Neutron Science, IFF, Forschungszentrum Jülich, Outstation at FRM II, Lichtenbergstrasse 1, D-85747 Garching, Germany*

<sup>5</sup>*Institut für Festkörperforschung, Forschungszentrum Jülich, D-52425 Jülich, Germany*

<sup>6</sup>*Frontier Research Center, Tokyo Institute of Technology, 4259 Nagatsuta-cho, Midori-ku, Yokohama 226-8503, Japan*

<sup>7</sup>*European Synchrotron Radiation Facility, Boîte Postale 220, F-38043 Grenoble, France*

(Received 14 July 2010; revised manuscript received 1 December 2010; published 9 February 2011)

We report on high-pressure powder synchrotron x-ray diffraction studies on  $M\text{Fe}_2\text{As}_2$  ( $M = \text{Ba}, \text{Ca}$ ) over a range of temperatures and pressures up to about 56 GPa using a membrane diamond-anvil cell. Our data indicate a phase transition to a collapsed tetragonal phase in both compounds upon compression. The data at 300 K are measured in both pressure-increasing and -decreasing cycles. Our measurements show that at 300 K in the Ba compound, the transition occurs at 27 GPa, which is much higher than the transition pressure of 1.7 GPa in the Ca compound. At low temperature, we could obtain data only in the pressure-increasing cycle, therefore a precise transition pressure is not identified. At a low temperature of 33 K, the transition to the tetragonal phase in the Ba compound starts, upon compression, at about 29 GPa, which is much higher than the transition pressure of 0.3 GPa at 40 K as known in the case of the Ca compound. The much higher transition pressure in the Ba compound may be due to its larger unit-cell volume at ambient pressure. It is important to note that the transition in both compounds occurs when they are compressed to almost the same value of the unit-cell volume and attain similar  $c_t/a_t$  ratios. We also show that the  $\text{FeAs}_4$  tetrahedra are much less compressible and more distorted in the collapsed tetragonal phase than their nearly regular shape in the ambient pressure phase. We present a detailed analysis of the pressure dependence of the structures as well as equations of state in these important  $\text{BaFe}_2\text{As}_2$  and  $\text{CaFe}_2\text{As}_2$  compounds.

DOI: [10.1103/PhysRevB.83.054503](https://doi.org/10.1103/PhysRevB.83.054503)

PACS number(s): 74.70.-b, 61.50.Ks, 72.80.Ga

## I. INTRODUCTION

The iron-based superconductors  $L_n\text{FeAs}(\text{O}_{1-x}\text{F}_x)$  ( $L_n =$  lanthanides) and oxygen-free doped  $M\text{Fe}_2\text{As}_2$  ( $M = \text{Ba}, \text{Ca}, \text{Sr}, \text{Eu}$ ),  $\text{LiFeAs}$ ,  $\text{FeSe}$ , and  $\text{SrFeAsF}$  have stimulated a great deal of activity<sup>1–37</sup> on superconductors derived from antiferromagnetic parent compounds. This novel class of materials, in addition to existing cuprate-based high- $T_c$  superconductors, provides yet another system for exploring the interplay between superconductivity and antiferromagnetism. The parent  $M\text{Fe}_2\text{As}_2$  compounds containing  $\text{FeAs}$  layers exhibit structural<sup>5</sup> and magnetic phase transitions<sup>5–7</sup> associated with Fe moments. For example,  $\text{BaFe}_2\text{As}_2$  undergoes structural (tetragonal-to-orthorhombic) and magnetic [paramagnetic-to-antiferromagnetic (AF)] phase transitions simultaneously at  $T_s \sim 140$  K.

Electron or hole doping into the parent compounds suppresses the structural and magnetic instabilities and induces superconductivity. For example, K-doped  $\text{BaFe}_2\text{As}_2$  ( $\text{Ba}_{0.55}\text{K}_{0.45}\text{Fe}_2\text{As}_2$ ) shows a  $T_c$  as high as 38 K,<sup>2</sup> while Co-doped  $\text{BaFe}_2\text{As}_2$  ( $\text{BaFe}_{1.8}\text{Co}_{0.2}\text{As}_2$ ) exhibits a  $T_c$  of 22 K.<sup>28</sup> The magnetic order can also be suppressed in the parent compound by the application of pressure, resulting in the appearance of superconductivity.<sup>3,30</sup> Thus, superconductivity in the parent  $\text{FeAs}$ -based compounds can be induced by either chemical substitution or application of external pressure. Chemical substitution generates charge carriers as well as chemical pressure due to the difference in size of the atoms,

for example, substitution of  $\text{Ba}^{2+}$  by  $\text{K}^+$  in  $\text{Ba}_{0.55}\text{K}_{0.45}\text{Fe}_2\text{As}_2$  (Ref. 2) and  $\text{Co}^{+2}$  by  $\text{Fe}^{+2}$  in  $\text{BaFe}_{1.8}\text{Co}_{0.2}\text{As}_2$ .<sup>28</sup> Both the chemical substitution as well as the external pressure lead to structural distortions. All these indicate a strong competition between the structural distortions, magnetic ordering, and superconductivity. The detailed interplay between these has hardly been understood up to now, which is due, to some extent, to the lack of precise structural data at high pressures. In addition, an important clue to the mechanism of superconductivity should be provided by high-pressure experiments on a stoichiometric sample since the application of pressure introduces no disorder. However, fundamental problems remain to be solved, as the appearance of pressure-induced superconductivity in  $M\text{Fe}_2\text{As}_2$  is highly sensitive<sup>4,21,22</sup> to pressure homogeneity.

In  $\text{CaFe}_2\text{As}_2$ , detailed neutron and x-ray diffraction analysis shows<sup>12,13</sup> that the system undergoes a first-order phase transition from a magnetic orthorhombic to a nonmagnetic “collapsed” tetragonal phase at  $P = 0.3$  GPa,  $T = 40$  K. The inclusion of only a small amount of tetragonal phase gives rise to a spurious superconductivity in the magnetic orthorhombic phase. A superconducting phase has been found<sup>30,31,33</sup> in a collapsed tetragonal structure of  $\text{CaFe}_2\text{As}_2$  with the disappearance of magnetism. However, the possible appearance of superconductivity in the collapsed tetragonal phase of  $\text{CaFe}_2\text{As}_2$  is presently under debate.<sup>4</sup> The application of uniaxial pressure along the  $c$  axis of a  $\text{CaFe}_2\text{As}_2$  single crystal shows<sup>34</sup> that the

room-temperature tetragonal phase can be stabilized at low temperatures for pressures above 0.06 GPa. Simultaneous resistivity measurements show that the phase is superconducting with a  $T_c$  of about 10 K. These measurements were performed in a limited pressure range ( $<2.0$  GPa).<sup>12,13,30,31,33,34</sup> In the case of  $\text{BaFe}_2\text{As}_2$ , the superconducting dome evolves<sup>2,3,14,21,32</sup> in a gradual way with the change of pressure (chemical or external), and superconductivity has been reported to exist in the orthorhombic structure, suggesting the coexistence of superconductivity and magnetic order. Although great efforts have been devoted to understanding the relationship between magnetism, lattice instability, and superconductivity, there are still some discrepancies and unclear issues. Recently, high-pressure measurements carried out<sup>16</sup> for  $\text{EuFe}_2\text{As}_2$  at 300 K showed a tetragonal to collapsed tetragonal phase transition at about 8 GPa.

External pressure has been found to play an important role in tailoring the  $T_c$  of the recently discovered FeAs-based superconductors. The parent 122-type FeAs compounds have been found to become superconductors<sup>3,30</sup> under high pressure. The response of pressure on  $T_c$  is found to be complex. The  $T_c$  of F-doped  $\text{LaOFeAs}$  was increased<sup>35</sup> from 26 to 43 K upon application of pressures of about 4 GPa. Pressure seems to suppress or enhance  $T_c$  depending<sup>36,37</sup> on the composition of the materials and their doping level. The chemical and external pressures are found to play<sup>14</sup> similar roles in leading to superconductivity, while also suppressing the tetragonal-to-orthorhombic phase transition and reducing the As-Fe-As bond angle and Fe-Fe distance. In particular,  $T_c$  is found to increase as the As-Fe-As bond angles tend toward the ideal tetrahedral value of  $109.47^\circ$ .

Spin fluctuations<sup>25,29</sup> were also suggested to play an important role in stabilizing the superconducting ground state. Extensive studies of phonon dynamics<sup>8–11</sup> suggest that it is unlikely that the superconductivity in iron pnictides is due to simple electron-phonon coupling. First-principles band-structure calculations have been used<sup>25</sup> to understand the relationship between the crystal structure, charge doping, and magnetism in  $\text{BaFe}_2\text{As}_2$  and  $\text{CaFe}_2\text{As}_2$ . Recently, *ab initio* molecular-dynamics<sup>26,27</sup> calculations have also been used to investigate the mechanism of electronic and structural phase transformation in  $\text{BaFe}_2\text{As}_2$  and  $\text{CaFe}_2\text{As}_2$  under pressure. The authors report that the structural phase transition from orthorhombic to tetragonal symmetry is accompanied by a magnetic phase transition in all the compounds while the nature of the transition is different for the two systems.

It is interesting to note that most of the high-temperature superconductors have a layered structure. It is also important to know how pressure changes the interaction between the layers, which can be directly determined from the measurement of the compressibility of the lattice parameters. We have investigated the pressure effects on  $\text{CaFe}_2\text{As}_2$  and  $\text{BaFe}_2\text{As}_2$  using the synchrotron x-ray diffraction technique. For  $\text{CaFe}_2\text{As}_2$ , Rietveld analysis of powder synchrotron data clearly suggests that it undergoes a phase transformation from a tetragonal to a collapsed tetragonal phase via an orthorhombic phase at very low pressures, as is well known from the literature. Powder synchrotron diffraction data do not show any appreciable change as pressure is increased up to  $\sim 37$  GPa at 40 K. The compound remains in the collapsed

tetragonal phase. On the other hand,  $\text{BaFe}_2\text{As}_2$  undergoes a tetragonal-to-orthorhombic phase transition around 130 K at about 1.3 GPa and remains in that phase upon lowering the temperature down to 33 K. An increase in pressure (at 33 K) results in a broadening of the diffraction profile at about 29 GPa. Detailed Rietveld analysis of the diffraction data clearly indicates the coexistence of orthorhombic and collapsed tetragonal phases above 29 GPa at 33 K. The phase fraction of the collapsed tetragonal phase increases with pressure. We have used helium as a pressure-transmitting medium, which provides the best hydrostatic conditions.<sup>38</sup> However, minor nonhydrostatic pressure conditions may influence the measurements and lead to extended coexisting orthorhombic and collapsed tetragonal phases over a wide pressure range at 33 K. The experiments could not be performed upon decreasing pressure at 33 K, therefore the precise transition pressure is not identified at low temperature. Upon heating from 33 to 300 K (at  $\sim 34$  GPa), we found that  $\text{BaFe}_2\text{As}_2$  is fully transformed into the collapsed tetragonal phase. Finally, at 300 K, while lowering the pressure,  $\text{BaFe}_2\text{As}_2$  is transformed again back to the tetragonal phase at about 20 GPa. In addition to this, high-pressure data were also collected for both compounds up to about 56 GPa at 300 K, indicating a tetragonal to collapsed tetragonal phase transition in  $\text{BaFe}_2\text{As}_2$  at about 27 GPa. The details of the measurements are given in Sec. II, results and discussion are presented in Sec. III, and conclusions are given in Sec. IV.

## II. EXPERIMENTAL

$M\text{Fe}_2\text{As}_2$  ( $M$ : Ba, Ca) samples were prepared by a solid-state reaction of  $M\text{As}$  ( $M = \text{Ca, Ba}$ ) and  $\text{Fe}_2\text{As}$ :  $M\text{As} + \text{Fe}_2\text{As} \rightarrow M\text{Fe}_2\text{As}_2$ .  $M\text{As}$  compounds were synthesized by heating  $M$  shots (99.99 wt%) with As powder (99.9999 wt%) at  $650^\circ\text{C}$  for 10 h in an evacuated silica tube.  $\text{Fe}_2\text{As}$  was synthesized from powders of mixed elements at  $800^\circ\text{C}$  for 10 h (Fe, 99.9 wt%). These products were then mixed by agate mortar in stoichiometric ratios, pressed, and heated in evacuated silica tubes at  $900^\circ\text{C}$  for 10 h to obtain sintered pellets. All the starting material preparation procedures were carried out in an argon-filled glove box ( $\text{O}_2, \text{H}_2\text{O} < 1$  ppm).

The x-ray powder diffraction measurements were carried out at the ID-27 beam line at the European Synchrotron Radiation Facility (ESRF, Grenoble, France). An applied pressure was generated by membrane diamond-anvil cells (DAC's). A powdery sample  $\sim 30\text{--}40\ \mu\text{m}$  in diameter and  $10\ \mu\text{m}$  in thickness was situated in the center of the diamond anvil's tip. Pressure was generated upon a stainless-steel gasket preindented to a  $40\text{--}50\ \mu\text{m}$  thickness, with a central hole of  $150\ \mu\text{m}$  in diameter filled with helium as the pressure-transmitting medium. The pressure was determined using the shift of the fluorescence line of the ruby. The wavelength of the x ray ( $0.3738\ \text{\AA}$ ) was selected and determined using a Si(111) monochromator and the iodine K edge. Then the sample to image plate (MAR345) detector distance was refined using the diffraction data of Si. A continuous helium flow CF1200 DEG Oxford cryostat was used to cool down the DAC. Special care was taken to obtain stable temperature and pressure conditions prior

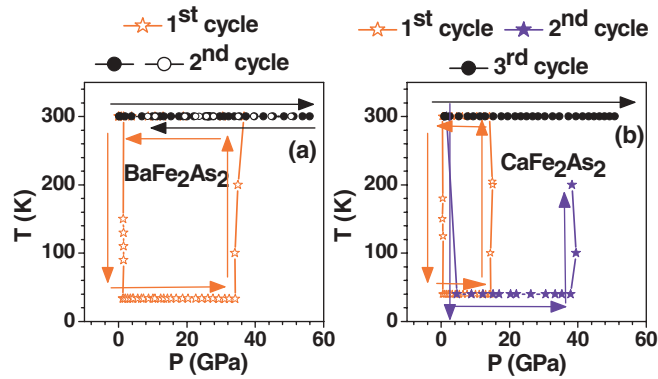


FIG. 1. (Color online) The pressure-temperature conditions for measurements of  $\text{BaFe}_2\text{As}_2$  and  $\text{CaFe}_2\text{As}_2$ . The circles, squares, and stars represent experimental data points in different cycles of our measurements. The solid and open circles correspond to the data points for  $\text{BaFe}_2\text{As}_2$  in the second cycle of measurements with increasing and decreasing pressure, respectively. The solid lines through the symbols are guides to the eye. Arrows indicate the sequence of measurements during the experiment.

to each acquisition. The precision and accuracy of the temperature measurement are better than 0.1 and 0.2 K, respectively. In the first cycle, the  $\text{BaFe}_2\text{As}_2$  and  $\text{CaFe}_2\text{As}_2$  samples were first cooled to 33 and 40 K, respectively, and then pressure was increased to  $\sim 35$  GPa. At 35 GPa, the temperature was slowly increased to 300 K. Finally, pressure was released at 300 K. Another set of measurements was carried out at ambient temperature (300 K) for both samples, where data were collected up to about 56 and 51 GPa for  $\text{BaFe}_2\text{As}_2$  and  $\text{CaFe}_2\text{As}_2$ , respectively. Typical exposure times of 20 seconds were employed for the measurements.

The two-dimensional powder images were integrated using the program FIT2D (Ref. 39) to yield intensity versus  $2\theta$  plot. As shown in Fig. 1, the high-pressure data for  $\text{BaFe}_2\text{As}_2$  (at 33 and 300 K) and  $\text{CaFe}_2\text{As}_2$  (at 40 and 300 K) have been measured in different cycles. For these measurements, samples have been loaded in four different DAC's. The diffraction patterns indicate preferred orientation of the sample along [103] for  $\text{BaFe}_2\text{As}_2$  at 300 K. On the other hand, the  $\text{CaFe}_2\text{As}_2$  sample showed preferred orientation along [213] and [200] in separate experiments at 40 and 300 K, respectively. Preferred orientation of crystal grains is observed along different axes in different loadings, which is common in high-pressure experiments. The structural refinements were performed using the Rietveld refinement program FULLPROF.<sup>40</sup> In all the refinements, the background was defined by a sixth-order polynomial in  $2\theta$ . A Thompson-Cox-Hastings pseudo-Voigt with axial divergence asymmetry function was chosen to define the profile shape for the powder synchrotron diffraction peaks. The scale factor, background, half-width parameters along with mixing parameters, lattice parameters, and positional coordinates were refined.

### III. RESULTS AND DISCUSSION

The powder synchrotron x-ray diffraction measurements for  $M\text{Fe}_2\text{As}_2$  ( $M = \text{Ba}, \text{Ca}$ ) at ambient conditions confirmed

a single-phase sample consistent with published reports.<sup>2,13</sup> The data were collected for  $M\text{Fe}_2\text{As}_2$  ( $M = \text{Ba}, \text{Ca}$ ) over a wide range of temperatures and pressures up to 56 GPa. The pressure-temperature conditions for measurement in various compression cycles for  $\text{BaFe}_2\text{As}_2$  and  $\text{CaFe}_2\text{As}_2$  are shown in Figs. 1(a) and 1(b), respectively.

#### A. High-pressure phase stability of $\text{BaFe}_2\text{As}_2$

Typical angle dispersive powder x-ray diffraction data collected for  $\text{BaFe}_2\text{As}_2$  at various pressures at 300 and 33 K are shown in Figs. 2 and 3. Figure 2(a) shows a portion of the diffraction patterns of  $\text{BaFe}_2\text{As}_2$  at selected pressures at 300 K during the pressure increase cycle. The diffraction profiles show dramatic changes with pressure. The Bragg peaks around  $2\theta = 10^\circ$  and  $13^\circ$  come close to each other with increasing pressure and finally merge at about 26 GPa. Upon a further increase of pressure, the Bragg peaks are again well separated for pressures above 34 GPa. Detailed Rietveld refinement of the powder diffraction data shows that diffraction patterns at 300 K (Table I) could be indexed using the tetragonal structure (space group  $I4/mmm$ ) up to 56 GPa. The fit between the observed and calculated profiles is quite satisfactory and some of them are shown in Fig. 2(b).

Earlier energy-dispersive x-ray diffraction carried out up to 22 GPa indicated<sup>15</sup> a tetragonal-to-orthorhombic phase transition for  $\text{BaFe}_2\text{As}_2$  at about 17 GPa at 300 K using a structure-free model. In view of this, we have also carried out Rietveld refinement of powder synchrotron data at 22 GPa (similar to Ref. 15) with an orthorhombic space group  $Fmmm$ . We have not found any substantial improvement in  $\chi^2$  with the orthorhombic phase refinement. The difference in the orthorhombic  $a_o$  and  $b_o$  lattice parameters is found to be less than 0.5%. However, Ref. 15 reported a difference of more than 3% in the values of the  $a_o$  and  $b_o$  lattice parameters. Thus, we refined the powder-diffraction data using a tetragonal

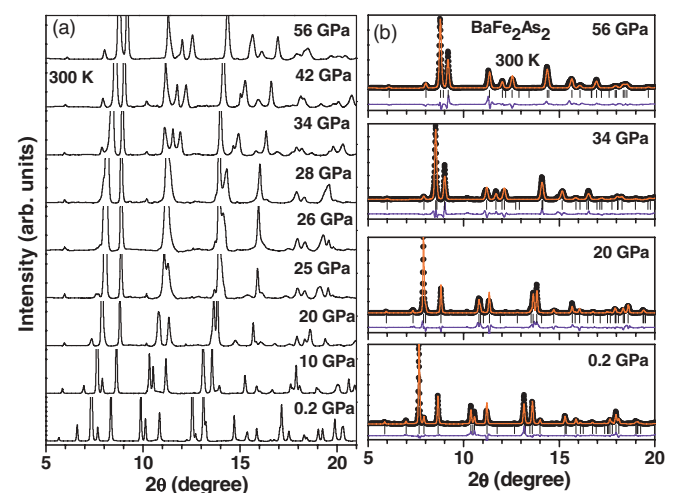


FIG. 2. (Color online) (a) Evolution of the powder synchrotron x-ray diffraction patterns of  $\text{BaFe}_2\text{As}_2$  at 300 K. (b) Observed (solid black circle), calculated (continuous red line), and difference (bottom blue line) profiles obtained after the Rietveld refinement of x-ray diffraction patterns of  $\text{BaFe}_2\text{As}_2$  using tetragonal space group ( $I4/mmm$ ) at selected pressures at 300 K.

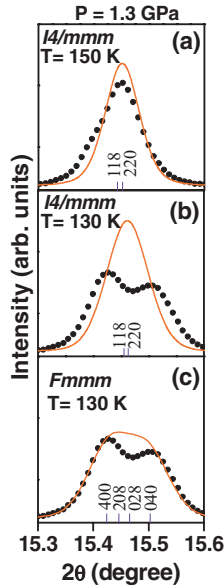


FIG. 3. (Color online) Tetragonal-to-orthorhombic phase transition in  $\text{BaFe}_2\text{As}_2$  at 1.3 GPa. The refinement of the diffraction pattern with (a,b) tetragonal phase (space group  $I4/mmm$ ) and (c) orthorhombic ( $Fmmm$ ) phase. The fitted profile clearly indicates a tetragonal-to-orthorhombic phase transition during cooling from 150 to 130 K at 1.3 GPa.

phase and believe that it undergoes a similar phase transition<sup>13</sup> as observed for  $\text{CaFe}_2\text{As}_2$ .

In another set of measurements, diffraction patterns were collected while lowering the temperature of the DAC at about 1 GPa. Detailed Rietveld analysis of the diffraction data reveals that it undergoes a tetragonal-to-orthorhombic phase transition upon cooling to 130 K at about 1.3 GPa, as shown in Fig. 3. The structure (Table I) was found to remain in the orthorhombic phase [Fig. 4(a)] down to 33 K at this pressure. An increase in pressure (at 33 K) results in a broadening of some of

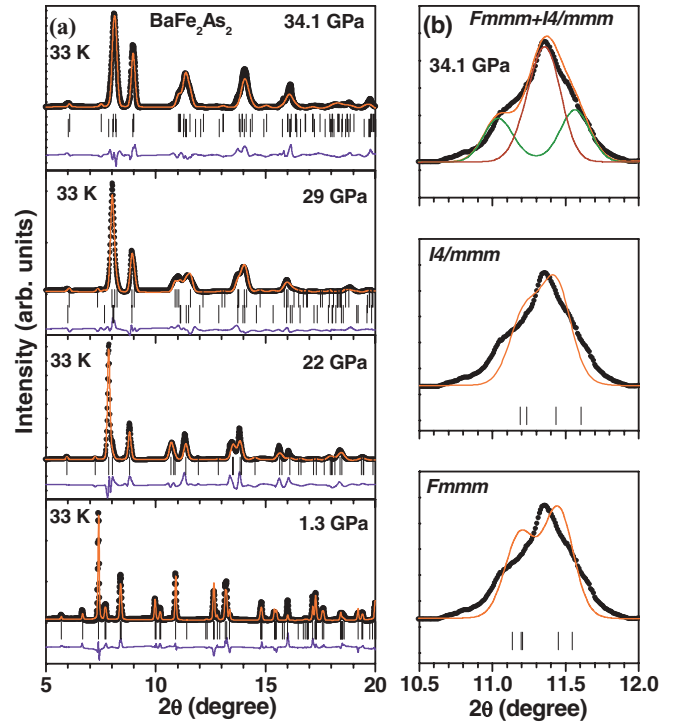


FIG. 4. (Color online) (a) Observed (solid black circle), calculated (continuous red line), and difference (bottom blue line) profiles obtained after the Rietveld refinement of  $\text{BaFe}_2\text{As}_2$ . The diffraction profiles at 1.3 and 22 GPa are refined using an orthorhombic phase (space group  $Fmmm$ ), while the profiles at 29 and 34.1 GPa are refined using a combination of tetragonal ( $I4/mmm$ ) and orthorhombic (space group  $Fmmm$ ) phases. Upper and lower vertical tick marks above the difference profiles at 29 and 34.1 GPa indicate peak positions of orthorhombic ( $Fmmm$ ) and tetragonal ( $I4/mmm$ ) phases, respectively. (b) The refinement of the diffraction pattern at 34.1 GPa and 33 K with an orthorhombic phase (space group  $Fmmm$ ), a tetragonal ( $I4/mmm$ ) phase, and a combination of tetragonal ( $I4/mmm$ ) and orthorhombic (space group  $Fmmm$ ) phases.

TABLE I. Refined results of the crystal structure for  $\text{BaFe}_2\text{As}_2$  at selected pressures and at temperatures of 300 and 33 K. Atomic positions for space group  $I4/mmm$ : Ba ( $2a$ ) (0 0 0), Fe ( $4d$ ) ( $1/2$  0  $1/4$ ), and As ( $4e$ ) (0 0  $z$ ). Atomic positions for space group  $Fmmm$ : Ba ( $4a$ ) (0 0 0), Fe ( $8f$ ) ( $1/4$ ,  $1/4$ ,  $1/4$ ), and As ( $8i$ ) (0 0  $z$ ). The measurements were carried out using a focused x-ray monochromatic beam of wavelength 0.3738 Å. The data collected up to  $20^\circ$  have been used to determine the reported parameters.

Temperature (K)	300	300	33	33
Pressure (GPa)	0.2	56	1.3	34.1
Space group	$I4/mmm$	$Fmmm$	$Fmmm$	$Fmmm+I4/mmm$
$a$ (Å)	3.9590(1)	3.7796(2)	5.5447(3)	5.2571(8)/3.7643(6)
$b$ (Å)	3.9590(1)	3.7796(2)	5.5773(3)	5.2738(9)/3.7643(6)
$c$ (Å)	13.005(3)	9.593(2)	12.852(6)	11.311(3)/10.828(3)
$V$ (Å <sup>3</sup> )	203.85(1)	137.07(1)	397.45(4)	313.70(7)/153.43(5)
$z$	0.3560(2)	0.3662(4)	0.3575(4)	0.3657(8)/0.3676(8)
R <sub>p</sub>	9.82	10.7	17.6	19.1
R <sub>wp</sub>	14.1	14.8	22.7	25.2
R <sub>exp</sub>	8.30	9.60	11.92	14.65
$\chi^2$	2.88	2.37	3.03	2.96
No. of reflections	78	56	66	60

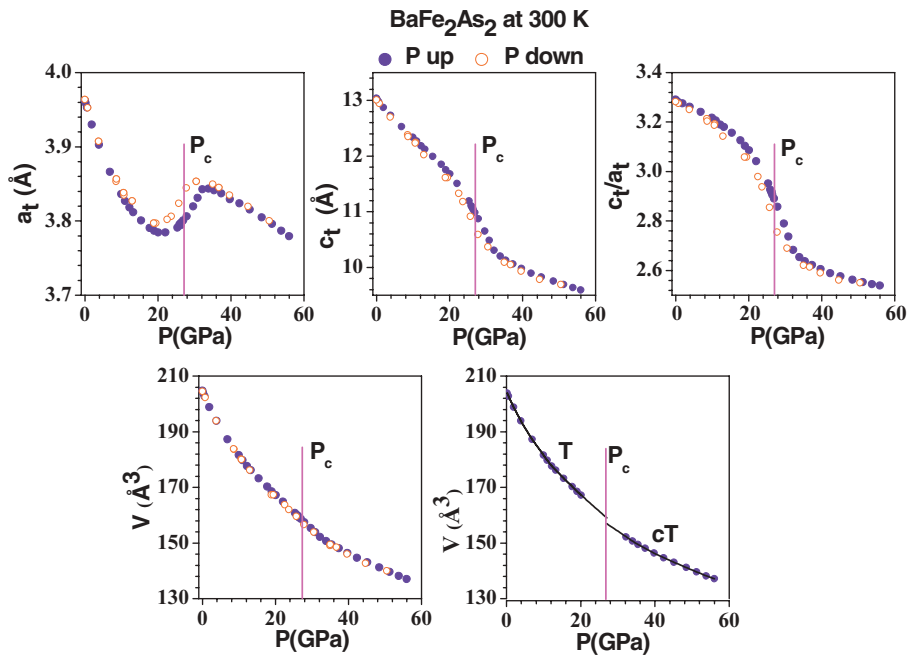


FIG. 5. (Color online) Pressure dependence of the structural parameters (lattice parameters, volume) and  $c_t/a_t$  of  $\text{BaFe}_2\text{As}_2$  at 300 K (tetragonal phase) in pressure-increasing ( $P$  up) and -decreasing ( $P$  down) cycles. The solid and open symbols correspond to the measurements in pressure-increasing and -decreasing cycles. The right-hand-side figure in the lower row shows fitting of pressure-volume data (pressure-increasing cycle) at 300 K to the third-order Birch-Murnaghan equation of state in the tetragonal ( $T$ ) and collapsed tetragonal ( $cT$ ) phase. The critical value of pressure ( $P_c$ ) for the phase transition at 300 K is 27 GPa. The critical value of pressure represents the average of the inflection points of the hysteresis loop.

the diffraction peaks [Fig. 4(a)] above 29 GPa. To account for the broadening, the diffraction data above 29 GPa were refined using an orthorhombic phase (space group  $Fmmm$ ), a tetragonal phase ( $I4/mmm$ ), and a combination of tetragonal and orthorhombic phases [Fig. 4(b)], respectively. Here we show an example [Fig. 4(b)] of such an analysis (Table I) for a measurement at 34.1 GPa and 33 K. The analysis of the diffraction data clearly indicates the presence of an additional tetragonal phase above 29 GPa. The coexistence of tetragonal and orthorhombic phases (Fig. 4) suggests an onset of the first-order phase transition at 29 GPa (at 33 K). The ratio of orthorhombic and tetragonal phases at 29 GPa is 74% and 26%, respectively. The percentage of the orthorhombic phase was found to decrease upon increasing the pressure up to 34.1 GPa (shown later in Fig. 6). Due to the experimental limitations, we could not increase pressure beyond 34.1 GPa at 33 K. During heating, the diffraction profiles were collected at 100 K (at 34.1 GPa), 200 K (at 34.9 GPa), and 300 K (36.7 GPa). The diffraction pattern at 300 K and 36.7 GPa could be indexed using only the collapsed tetragonal phase. Finally, the diffraction profiles were collected while lowering the pressure at 300 K. We noticed that below 20 GPa at 300 K, the collapsed phase reverted back to the ambient tetragonal phase.

The effects of pressure inhomogeneity on the phase-transition behavior of FeAs compounds have been discussed in the literature.<sup>21,22</sup> Recently, pressure-dependent electrical resistivity of  $\text{BaFe}_2\text{As}_2$  has been measured up to 16 GPa.<sup>21</sup> The liquid Fluorinert was used as a pressure-transmitting medium. Above 1.2 GPa, the solidification of Fluorinert may yield moderate inhomogeneous pressure distributions. Duncan *et al.*<sup>22</sup> have used three different pressure-transmitting media, namely pentane-isopentane, Daphne oil, and steatite, for measurements of electrical resistivity of  $\text{BaFe}_2\text{As}_2$  up to about 5 GPa. All these pressure media have their own intrinsic level of hydrostaticity and yield moderate inhomogeneous pressure distributions at very low pressures. The authors<sup>22</sup> find that the pressure-temperature phase diagram of  $\text{BaFe}_2\text{As}_2$  is

extremely sensitive to the pressure-transmitting medium used for the experiment and, in particular, to the level of resulting uniaxial stress. An increasing uniaxial pressure component in this system quickly reduces the spin-density-wave order and favors the appearance of superconductivity.

In the present measurements, we used helium as a pressure-transmitting medium, as it provides the best hydrostatic conditions.<sup>38</sup> During the measurements, we determined the pressure using two ruby balls. The pressure difference determined from ruby balls was always below 0.1–0.2 GPa. Nonhydrostaticity of the pressure cannot be completely ruled out at 33 K and may influence the results obtained from our studies on these compounds. The nonhydrostaticity may cause an extended coexistence of orthorhombic and collapsed tetragonal phases over a wide pressure range at 33 K and may also lead to a broadening of the diffraction peaks [Fig. 4(a)].

Figures 5 and 6 show the pressure dependence of the structural parameters (lattice parameters, volume, and  $c_t/a_t$ ) obtained from Rietveld refinements for  $\text{BaFe}_2\text{As}_2$  at 300 K (tetragonal phase) and 33 K (orthorhombic phase) in pressure-increasing and -decreasing cycles, respectively. For easy comparison, orthorhombic lattice parameters ( $a$ ,  $b$ , and  $c$ ) are converted into the equivalent tetragonal lattice parameters ( $a_{ot}$ ,  $b_{ot}$ , and  $c_{ot}$ ) using the relations  $a_{ot} = a/\sqrt{2}$ ,  $b_{ot} = b/\sqrt{2}$ , and  $c_{ot} = c$ . It is clear from Fig. 5 that upon increasing pressure at 300 K, the  $a$  lattice parameter first decreases (up to 22 GPa) and then increases (up to 32 GPa) and again further decreases up to 56 GPa. The  $c$  lattice parameter decreases with pressure in the entire range of our measurements.

We have fitted the pressure-volume data using the Birch-Murnaghan equation of state separately in the pressure range of 0–20 GPa (tetragonal phase) and 32–56 GPa (collapsed tetragonal phase) at 300 K. It can be clearly seen from Fig. 5 that the volume decreases by about 1.4% across the phase transition. Using a similar fitting procedure, at the transition, the  $a_t$  lattice parameter was found to increase (1.75%) with compression while  $c_t$  decreased (4.9%). The variation of

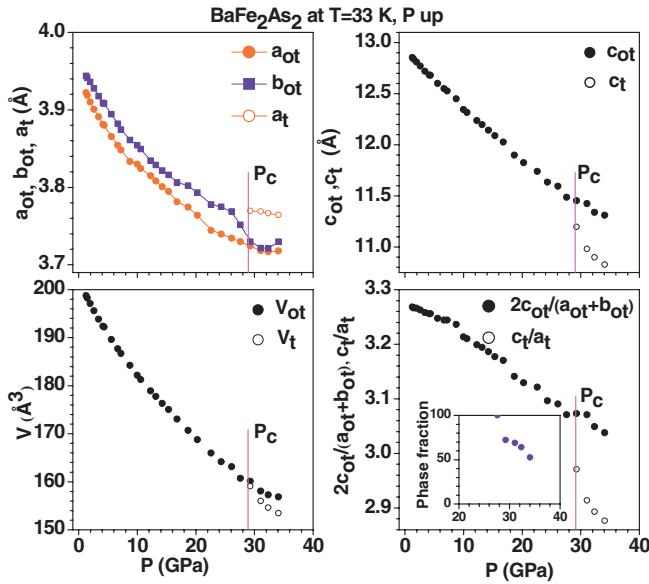


FIG. 6. (Color online) Pressure dependence of the structural parameters (lattice parameters, volume) and  $c_t/a_t$  of  $\text{BaFe}_2\text{As}_2$  at 33 K (in orthorhombic phase) in pressure-increasing ( $P$  up) cycle. For easy comparison, orthorhombic lattice parameters ( $a$ ,  $b$ , and  $c$ ) are converted into the equivalent tetragonal lattice parameters ( $a_{ot}$ ,  $b_{ot}$ , and  $c_{ot}$ ) using the relations  $a_{ot} = a/\sqrt{2}$ ,  $b_{ot} = b/\sqrt{2}$ , and  $c_{ot} = c$ . The open symbols above 29 GPa correspond to the structural data ( $a_t$ ,  $c_t$ , and  $c_t/a_t$ ) in the collapsed tetragonal phase. The percentage variation of orthorhombic phase during our measurements is shown in the inset of the lower row. The critical value of pressure ( $P_c$ ) for the phase transition at 33 K is 29 GPa.

$a_t$ ,  $c_t$ ,  $c_t/a_t$ , and  $V$  at 300 K in the pressure-increasing and -decreasing cycles (Fig. 5) clearly indicates hysteresis during the phase transition, and confirms the first-order nature of the phase transition. The critical value of pressure for the phase transition is 27 GPa as obtained from the average of the inflection points of the hysteresis loop. Similar observations have already been seen for  $\text{CaFe}_2\text{As}_2$ .<sup>12,13</sup> The variation of volume and  $c_t/a_t$  as a function of  $P/P_c$  ( $P$  and  $P_c$  are the values of the applied and phase-transition pressure, respectively) in both  $\text{BaFe}_2\text{As}_2$  and  $\text{CaFe}_2\text{As}_2$  (Fig. 7) appears to be nearly identical. X-ray diffraction measurements for  $\text{CaFe}_2\text{As}_2$  show<sup>12,13</sup> that during the structural phase transition from the

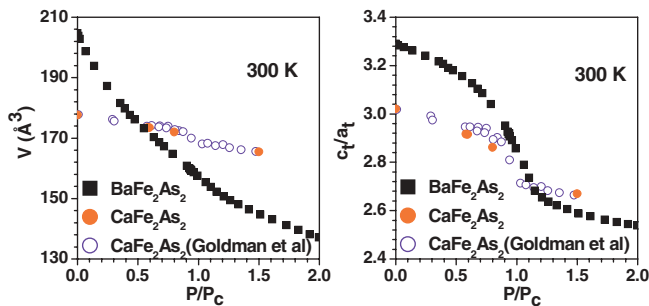


FIG. 7. (Color online) Volume and  $c_t/a_t$  as a function of  $P/P_c$  at 300 K. The  $P_c$  values at 300 K are 27 and 1.7 GPa for  $\text{BaFe}_2\text{As}_2$  and  $\text{CaFe}_2\text{As}_2$ , respectively. The experimental data for  $\text{CaFe}_2\text{As}_2$  as published by Goldman *et al.* (Ref. 13) are also shown by open circles.

tetragonal to the collapsed phase, the  $c_t$  lattice parameter contracts by about 9%, whereas  $a_t$  expands by about 1.5%. Furthermore, in  $\text{CaFe}_2\text{As}_2$  there is a continuous evolution of  $c_t/a_t$  as a function of pressure. The authors of Refs. 12 and 13 have not reported any phase coexistence during the transition from the tetragonal to the collapsed tetragonal phase. However, there is a small hysteresis in the  $a_t$ ,  $c_t$ , and  $c_t/a_t$  values. Similar behavior has been found in our measurements (Fig. 5) for  $\text{BaFe}_2\text{As}_2$ .

Similar to  $\text{CaFe}_2\text{As}_2$ ,<sup>12,13</sup> observation of a hysteresis in the variation of lattice parameters in the pressure-increasing and -decreasing cycles of  $\text{BaFe}_2\text{As}_2$  at 300 K, across the tetragonal to collapsed tetragonal phase transition, suggest a first-order nature of the phase transition. On the other hand, at 33 K the lattice parameters, volume, and  $2c_{ot}/(a_{ot} + b_{ot})$  (equivalent tetragonal values) are found to decrease (Fig. 6) with increasing pressure. Above 29 GPa, we found a coexistence of orthorhombic and tetragonal phases. It is interesting to note that the transition to the collapsed phase in  $\text{BaFe}_2\text{As}_2$  occurs at nearly the same volume of about  $165 \text{ \AA}^3$  on compression at 300 or 33 K.

The data for  $\text{BaFe}_2\text{As}_2$  have been measured in both the pressure-increasing and -decreasing cycles at 300 K. The critical value of pressure for the phase transition is 27 GPa as obtained from the average of the inflection points of the hysteresis loop. However, at 33 K measurements were carried out only in a pressure-increasing cycle. The coexistence of tetragonal and orthorhombic phases (Fig. 4) suggests an onset of the phase transition at 29 GPa (at 33 K). Hysteresis effects have already been seen for the transition to the collapsed phase in  $\text{CaFe}_2\text{As}_2$ .<sup>12,13</sup> The nonhydrostatic pressure conditions<sup>21,22</sup> may also influence the measurements. We find that at the highest pressure of 34.1 GPa (at 33 K) there is still 50% of the orthorhombic phase (Fig. 6), implying that the full width of the transition regime is of the order of 10 GPa. However, since the complete hysteresis loop with decreasing pressure could not be measured at 33 K, the precise transition pressure is not identified at low temperature. It should be noted that in the case of  $\text{CaFe}_2\text{As}_2$ ,<sup>12,13</sup> the collapsed tetragonal phase transition occurs at a lower pressure (0.3 GPa) at a low temperature (50 K) in comparison to 1.7 GPa at 300 K.

For comparison, the results from *ab initio* molecular-dynamics (MD) simulations<sup>26</sup> are also shown along with the low-temperature experimental data (Fig. 8). The simulations were carried out at zero temperature. As discussed earlier, the coexistence of the tetragonal and orthorhombic phases in the experimental data for  $\text{BaFe}_2\text{As}_2$  at 33 K suggests an onset of the phase transition at 29 GPa, while  $\text{CaFe}_2\text{As}_2$  is known to show<sup>12,13</sup> a transition to the collapsed phase at 0.3 GPa at 40 K. We have measured high-pressure data in the collapsed phase of  $\text{CaFe}_2\text{As}_2$  at and above 0.45 GPa at 40 K. The calculated transition pressure values for the orthorhombic-to-tetragonal phase transition from MD simulations are 17.5 and 5.25 GPa for  $\text{BaFe}_2\text{As}_2$  and  $\text{CaFe}_2\text{As}_2$ , respectively. There is a good qualitative agreement (Fig. 8) between our experimental data and the simulations. The simulations show a first-order orthorhombic to collapsed tetragonal transition in  $\text{CaFe}_2\text{As}_2$  that is in agreement with the experimental data. For  $\text{BaFe}_2\text{As}_2$ , MD simulations show a continuous orthorhombic-to-tetragonal phase transition, unlike the first-order phase

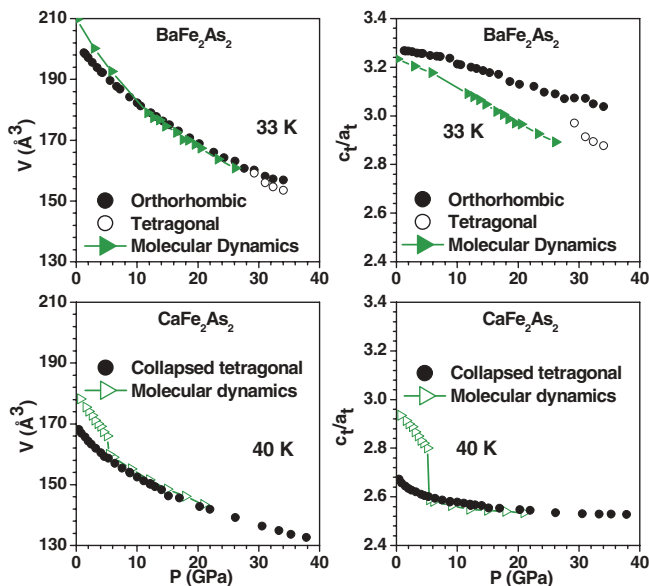


FIG. 8. (Color online) Comparison between the experimental data and molecular-dynamics simulations<sup>26</sup> for  $\text{BaFe}_2\text{As}_2$  and  $\text{CaFe}_2\text{As}_2$  at low temperatures. The solid lines through the symbols are guides to the eye. The coexistence of tetragonal and orthorhombic phases in  $\text{BaFe}_2\text{As}_2$  suggests the onset of the phase transition at 29 GPa (at 33 K), while  $\text{CaFe}_2\text{As}_2$  is known to show<sup>12,13</sup> a transition to the collapsed phase at 0.3 GPa at 40 K. We have measured high-pressure data in the collapsed phase of  $\text{CaFe}_2\text{As}_2$  at and above 0.45 GPa at 40 K. The calculated critical pressure values for the orthorhombic-to-tetragonal phase transition from molecular-dynamics simulations are 17.5 GPa (at 0 K) and 5.25 GPa (at 0 K), respectively, for  $\text{BaFe}_2\text{As}_2$  and  $\text{CaFe}_2\text{As}_2$ .

transition as observed in our experiments. The simulations overestimate<sup>26</sup> the unit-cell volume and magnetic moment of Fe for the FeAs compounds. The interplay among electronic, magnetic, and lattice dynamics influences the phase transition in FeAs compounds. The overestimation of the unit-cell volume causes the transition to the collapsed phase to occur at a higher pressure as in MD simulations.

Recently, the temperature dependence of the electrical resistivity of  $\text{BaFe}_2\text{As}_2$  was measured under pressure up to 16 GPa by Yamazaki *et al.*<sup>21</sup> Measurements were performed upon cooling at fixed values of pressures. The antiferromagnetic ordering temperature was found to decrease with increasing pressure. The magnetic ordering was found to completely suppress at 10.5 GPa. In our measurements, the sample has been first cooled from 300 to 33 K at 1.3 GPa. During cooling of the sample, we find that  $\text{BaFe}_2\text{As}_2$  undergoes a tetragonal-to-orthorhombic phase transition (Fig. 3) at 130 K (at 1.3 GPa). The observation is in agreement with the data of Yamazaki *et al.*<sup>21</sup> Further, the orthorhombic phase sample, compressed to high pressures, showed a transition to a tetragonal phase at 29 GPa (at 33 K). In general, the phase transitions are strongly influenced by the thermodynamic history (pressure and temperature) of the sample. The phase-transition behavior of  $\text{BaFe}_2\text{As}_2$  seems to depend strongly on the pressure and temperature conditions. The difference in compression conditions of samples as observed in our

experiment and that of Yamazaki *et al.* may cause different phase-transition behavior.

The electronic properties of the FeAs superconductors are sensitively controlled by distortions of the  $\text{FeAs}_4$  tetrahedra in terms of As-Fe-As bond angle and Fe-As bond length. The pressure dependence of the As-Fe-As bond angle and the As-Fe bond length of  $\text{BaFe}_2\text{As}_2$  at 300 K (tetragonal phase) and 33 K (orthorhombic phase) is shown in Fig. 9. It is clear from this figure that at 300 K (in the tetragonal phase), the two As-Fe-As bond angles were close to the ideal tetrahedral value of  $109.47^\circ$ . However, with an increase of pressure, the deviation from the ideal tetrahedral angle increases. There is an anomalous increase in the difference between the two As-Fe-As bond angles starting at about 10 and 22 GPa [Fig. 9(a)]. The latter anomaly can be associated with the structural transition to the collapsed phase. However, lattice parameters do not indicate any appreciable change at about 10 GPa. The anomaly in the As-Fe-As bond angles at 10 GPa could have an electronic origin.

*Ab initio* calculations<sup>20</sup> also show that the strong interaction between As ions in FeAs compounds is controlled by the Fe-spin state. Reducing the Fe-magnetic moment weakens the Fe-As bonding and, in turn, increases the As-As interactions. The loss of Fe moment at 10.5 GPa in  $\text{BaFe}_2\text{As}_2$  (Ref. 22) may increase the As-As interaction along the  $c$  axis. This, in turn, would change the  $z$  parameter of the As atom and may lead to an increase in the distortion of the As-Fe-As bond angle (Fig. 9) at 10.5 GPa in our measurements at 33 K as well as at 300 K. Thus, the anomaly in the As-Fe-As bond angles at about 10 GPa and 33 K [Fig. 9(b)] in our experiment may be associated with the suppression of antiferromagnetic ordering as indicated by the resistivity measurements.<sup>21</sup>

As mentioned earlier, due to hysteresis effects and nonhydrostatic pressure conditions, the tetragonal-to-orthorhombic phase-transition pressure in  $\text{BaFe}_2\text{As}_2$  at 33 K is not exactly determined. However, the onset of the tetragonal transition

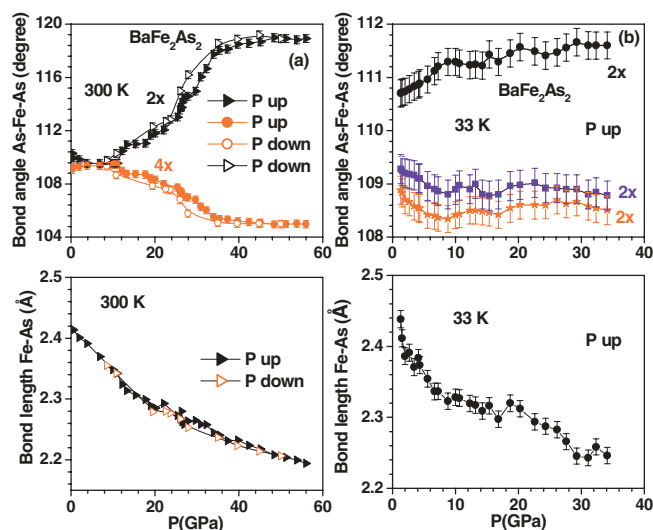


FIG. 9. (Color online) Pressure dependence of the As-Fe-As bond angle and As-Fe bond length of  $\text{BaFe}_2\text{As}_2$  at (a) 300 K (tetragonal phase) and (b) 33 K (in orthorhombic phase). The solid lines through the symbols are guides to the eye. The error bars at 300 K are comparable to the size of the symbol.

on increasing pressure at 29 GPa (at 33 K), as observed in our experiments (Fig. 4), is far above suppression of the magnetic ordering in  $\text{BaFe}_2\text{As}_2$  (Ref. 21) at 10.5 GPa at low temperature. Our measurement indicates a complete separation of the structural distortion and the antiferromagnetic ordering in  $\text{BaFe}_2\text{As}_2$ . Presently, there is a belief<sup>5,7</sup> that for 122 FeAs compounds there is a strong connection between the structural and magnetic phase transitions. However, for some 1111 FeAs compounds,<sup>6,24</sup> the structural and magnetic transitions do not occur at the same temperature. For example, in the case of  $\text{SrFeAsF}$ ,<sup>24</sup> upon cooling, the onset of the tetragonal-to-orthorhombic phase transition is at 180 K; however, the paramagnetic-to-antiferromagnetic phase transition takes place only upon further cooling of the orthorhombic phase at 133 K. It seems plausible that the structural distortion and the antiferromagnetic ordering in  $\text{BaFe}_2\text{As}_2$  at 33 K occur at different pressures. The inelastic neutron-scattering measurements<sup>23</sup> as well as *ab initio* calculations<sup>20</sup> show that spin fluctuations in FeAs compounds are present at all temperatures up to 300 K at ambient pressure. It is likely that the anomaly in the As-Fe-As bond angles at 10 GPa [Fig. 9(a)] may be due to suppression of paramagnetic spin fluctuations at 300 K.

It can be seen that in both phases at 300 K the compressibility along the  $a$  axis is smaller than that along the  $c$  axis. The pressure-volume data were fitted by a third-order Birch-Murnaghan equation of state to determine the bulk modulus  $B$  at zero pressure and its pressure derivative  $B'$ . The obtained parameters are  $B = 65.7 \pm 0.8$  GPa,  $B' = 3.9 \pm 0.1$  for the tetragonal phase (0–20 GPa) and  $B = 153 \pm 3$  GPa,  $B' = 1.8 \pm 0.1$  for the collapsed tetragonal phase (from fitting of data from 32–56 GPa) at 300 K. The  $B$  and  $B'$  values extracted from the pressure-volume relation in the orthorhombic phase (33 K, from fitting of data from 1 to 34 GPa) are  $82.9 \pm 1.4$  and  $3.4 \pm 0.1$  GPa, respectively. The fitted ambient pressure volumes for the tetragonal and collapsed tetragonal phase at 300 K are  $V_o = 204.3 \pm 0.1$  and  $181.6 \pm 0.7 \text{ \AA}^3$ , respectively. However,  $V_o$  for the orthorhombic phase at 33 K is  $201.78 \pm 0.13 \text{ \AA}^3$ . High-pressure x-ray diffraction experiments for  $\text{EuFe}_2\text{As}_2$  carried out at ambient temperature give bulk modulus values<sup>16</sup> of  $39.3 \pm 1.6$  and  $134.0 \pm 1.6$  GPa in the tetragonal and collapsed tetragonal phase, respectively. The bulk modulus value of  $\text{EuFe}_2\text{As}_2$  in the tetragonal phase is about 60% of the  $B$  value of  $\text{BaFe}_2\text{As}_2$ , whereas the  $B$  values in the collapsed phase of both compounds are nearly the same. Furthermore, we find that the value of  $B$  in the tetragonal phase of  $\text{BaFe}_2\text{As}_2$  is very close to that obtained from the high-pressure measurements<sup>18</sup> of  $\text{LaFeAsO}_{0.9}\text{F}_{0.1}$  ( $B = 78$  GPa).

The  $c_t/a_t$  ratio for  $\text{BaFe}_2\text{As}_2$  varies from 3.3 to 2.55 upon an increase of pressure to 56 GPa. It should be noted that  $c_t/a_t$  of the Ba compound reaches a value of 2.92 before the transition to the collapsed phase, which is nearly the same as for  $\text{CaFe}_2\text{As}_2$  at ambient pressure. However, in the case of  $\text{CaFe}_2\text{As}_2$ , the transition to the collapsed phase is at very low pressures of 1.7 GPa at 300 K. The  $\text{FeAs}_4$  tetrahedral volumes in the tetragonal phase at ambient conditions and in the orthorhombic phase at 33 K and 1 GPa are about  $22 \text{ \AA}^3$ . However, the collapsed transition at 300 K as well as 33 K starts when the  $\text{FeAs}_4$  tetrahedra are compressed (Fig. 10) below

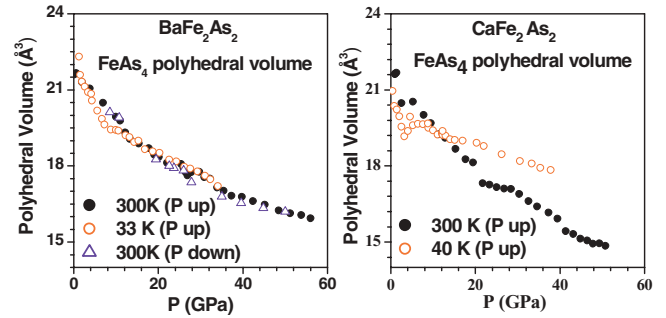


FIG. 10. (Color online) Pressure variation of  $\text{FeAs}_4$  tetrahedral volume in  $\text{BaFe}_2\text{As}_2$  and  $\text{CaFe}_2\text{As}_2$ .

about  $17.5 \text{ \AA}^3$ . We also found that the  $\text{FeAs}_4$  tetrahedra are much less compressible (Fig. 10) and are much more distorted in the collapsed phase compared to their nearly regular shape in the ambient pressure tetragonal phase.

### B. High-pressure phase stability of $\text{CaFe}_2\text{As}_2$

It is well established in the literature that at ambient pressure,  $\text{CaFe}_2\text{As}_2$  undergoes<sup>7</sup> a first-order transition from a high-temperature nonmagnetic tetragonal phase to an antiferromagnetic orthorhombic phase at  $T = 172$  K. The application of modest pressures ( $P > 0.23$  GPa) at low temperatures of about 40 K transforms the antiferromagnetic orthorhombic phase to a different nonmagnetically ordered collapsed tetragonal structure. The lattice parameters are found to change significantly as a function of pressure, with a dramatic decrease in both the unit-cell volume and the  $c_t/a_t$  ratio.

To explore the possibilities of a structural phase transition from a collapsed tetragonal to another phase with pressure, we carried out powder synchrotron diffraction experiments at high pressures. The sample was first cooled to 40 K at about 0.5 GPa. Once the temperature was stabilized at 40 K, the pressure was increased up to  $\sim 34$  GPa. The diffraction data (Fig. 11) do not show any appreciable change in all of the studied pressure range, that is,  $\text{CaFe}_2\text{As}_2$  remained in the collapsed tetragonal phase.

We also performed another experiment in which we collected powder-diffraction data at 300 K up to 51 GPa. The sample undergoes a structural phase transition (Fig. 11) into the collapsed phase at about 2 GPa. This observation is in agreement with that already reported in the literature.<sup>11–13</sup> The neutron and x-ray diffraction experiments<sup>11–13</sup> carried out up to 5 GPa show a similar transition from the tetragonal to the collapsed tetragonal phase at 1.7 GPa. As shown in Fig. 11, all the peaks in the diffraction profiles are well accounted for, using a collapsed tetragonal phase at the highest pressure. The relative intensity of Bragg peaks for scattering angles  $\sim 7.5^\circ - 9.5^\circ$  shows (Fig. 11) large changes upon an increase of pressure from 1 to 25 GPa at 300 K. These changes are associated with a collapsed phase transition (at 1.7 GPa) and gradual changes with increasing pressure. The profiles are well reproduced by the Rietveld refinements (Table II) of the structure that suitably include the variation in the atom positions and preferred orientation. Further, there is no signature of any post-collapsed phase transition in  $\text{CaFe}_2\text{As}_2$  up to 51 GPa ( $\sim 34$  GPa) at 300 K (40 K).



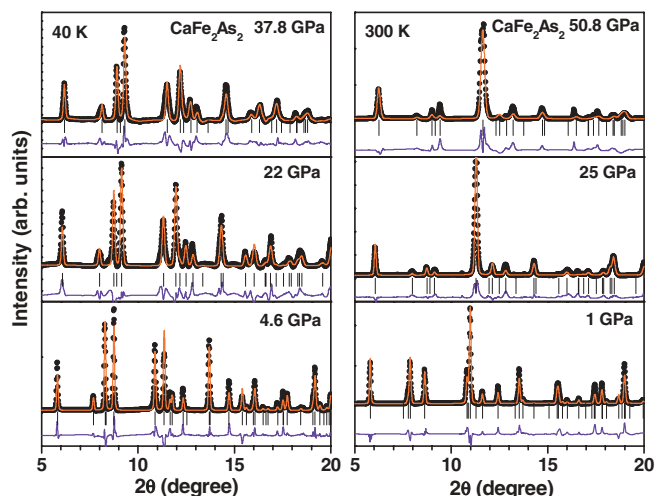


FIG. 11. (Color online) Observed (open circle), calculated (continuous line), and difference (bottom line) profiles obtained after the Rietveld refinement of  $\text{CaFe}_2\text{As}_2$  at selected pressures and 40 and 300 K. The diffraction profiles are refined using the tetragonal space group  $I4/mmm$ .

Figures 12 and 13 show the variation of lattice parameters,  $c_t/a_t$ , volume, As-Fe-As bond angle, and Fe-As bond length obtained from the Rietveld analysis of powder synchrotron diffraction data as a function of pressure in compression cycles (Fig. 1) of  $\text{CaFe}_2\text{As}_2$  at 40 and 300 K. We find that at 0.5 GPa and 40 K [Fig. 13(b)], the As-Fe-As bond angles show a deviation from the value of  $109.47^\circ$  for an ideal  $\text{FeAs}_4$  tetrahedron. A further increase of pressure up to 4 GPa shows an increase in deviation from the ideal tetrahedron angle indicating an increasing distortion of the  $\text{FeAs}_4$  tetrahedron in the collapsed phase. The deviation is found to decrease with a further increase of pressure up to 10 GPa, and then it remains almost constant up to the highest measured pressure of 37 GPa at 40 K. At 300 K, we find that in the parent tetragonal phase at 0.5 GPa and 300 K, the deviation of the As-Fe-As angles [Fig. 13(a)] is smaller than the deviation at a similar pressure at 40 K. As expected, the deviation was found to

TABLE II. Refined results of the crystal structure for  $\text{CaFe}_2\text{As}_2$  at selected pressures and at temperatures of 300 and 40 K. Atomic positions for space group  $I4/mmm$ : Ca ( $2a$ ) (0 0 0); Fe ( $4d$ ) ( $1/2$  0  $1/4$ ), and As ( $4e$ ) (0 0  $z$ ). The measurements were carried out using a focused x-ray monochromatic beam of wavelength 0.3738 Å. The data collected up to  $20^\circ$  have been used to determine the reported parameters.

Temperature (K)	300	300	40	40
Pressure (GPa)	1	50.8	4.6	37.8
Space group	$I4/mmm$	$I4/mmm$	$I4/mmm$	$I4/mmm$
$a = b$ (Å)	3.9052(1)	3.6727(3)	3.9396(1)	3.7439(3)
$c$ (Å)	11.402(2)	9.3173(5)	10.258(4)	9.4616(8)
$V$ (Å <sup>3</sup> )	173.88(2)	125.68(2)	159.22(3)	132.62(2)
$Z$	0.3726(4)	0.3843(7)	0.3690(2)	0.3726(3)
Rp	18.0	15.4	17.8	18.2
Rwp	22.5	20.6	22.3	24.1
R exp	12.62	12.85	12.95	14.77
$\chi^2$	3.18	2.58	2.95	2.65
No. of reflections	62	44	52	37

increase with an increase of pressure to 2 GPa at 300 K during the tetragonal to collapsed tetragonal phase transition. Upon a further increase of pressure, the As-Fe-As bond angle data show small anomalies (Fig. 13) at about 20 and 40 GPa. At present, we do not have any explanation for the origin of the previously mentioned anomalies in the As-Fe-As bond-angle data. High-pressure experiments on FeSe at ambient temperature also show<sup>19</sup> anomalous variations in the Se-Fe-Se bond angles at low pressures of 1 GPa. As explained earlier for  $\text{BaFe}_2\text{As}_2$ , the increases in the distortion of the bond angles are related to the suppression of the magnetic ordering. This may not be the reason for the anomalies in  $\text{CaFe}_2\text{As}_2$ , as we are already in the nonmagnetic<sup>12,13</sup> collapsed tetragonal phase of  $\text{CaFe}_2\text{As}_2$  above 1.7(0.3) GPa at 300(40) K.

It is also interesting to notice that the variation of the Fe-As bond length in the collapsed phase at 300 K shows a decrease of about 10% (Fig. 13) upon an increase of pressure from

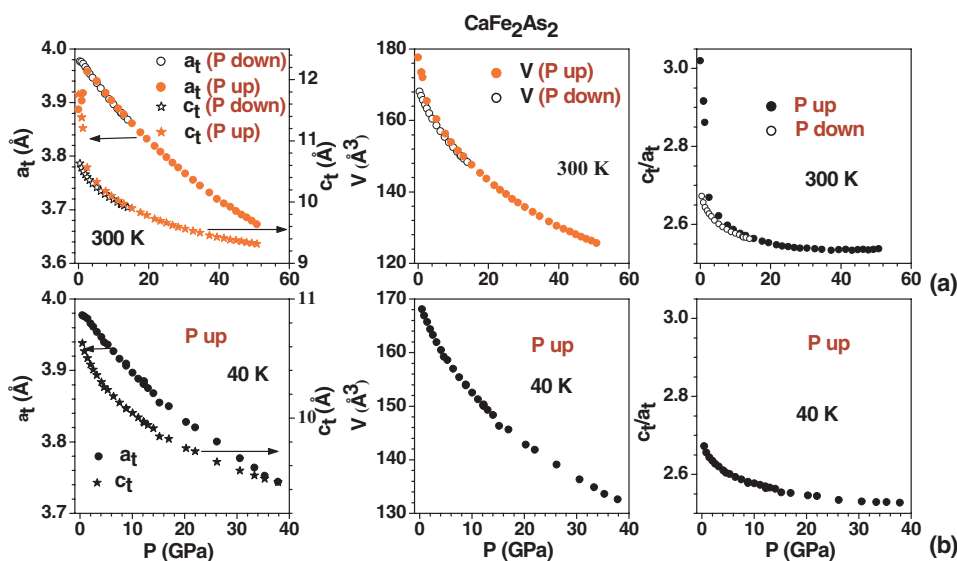


FIG. 12. (Color online) Pressure dependence of the structural parameters (lattice parameters, volume) and  $c_t/a_t$  of  $\text{CaFe}_2\text{As}_2$  at (a) 300 K and (b) 40 K in pressure-increasing ( $P$  up) and -decreasing ( $P$  down) cycles. Solid and open symbols correspond to the measurements in pressure-increasing and -decreasing cycles.

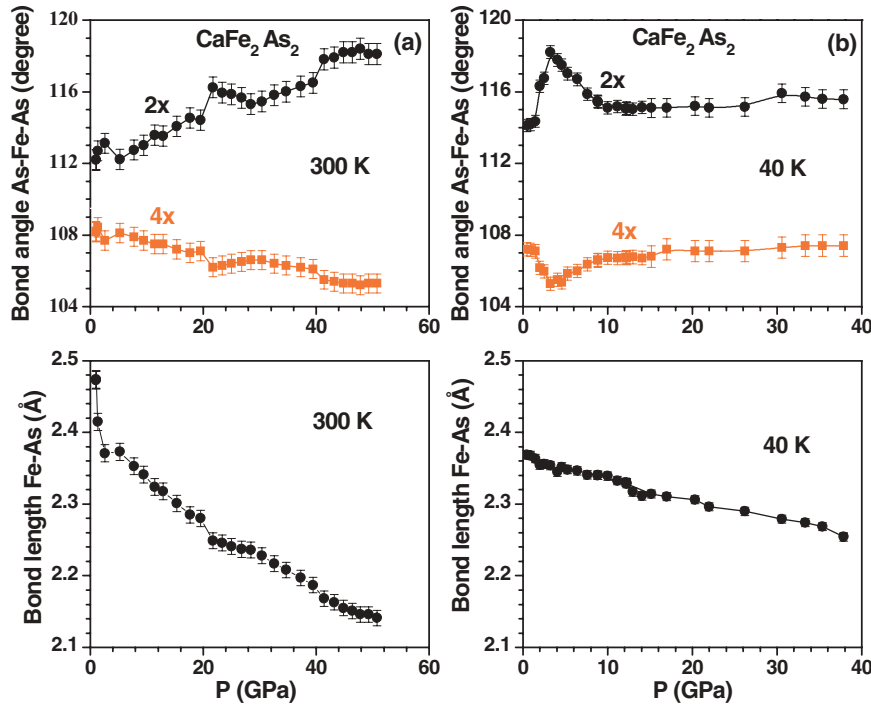


FIG. 13. (Color online) Pressure dependence of the As-Fe-As bond angle and As-Fe bond length of  $\text{CaFe}_2\text{As}_2$  at (a) 300 K and (b) 33 K, respectively. The bond angles are plotted only for data taken during pressure-increasing cycles at 300 and 33 K. The solid lines through the symbols are guides to the eye.

2 to 51 GPa. The pressure variation of  $\text{FeAs}_4$  tetrahedral volume in  $\text{CaFe}_2\text{As}_2$  is shown in Fig. 10. The transition to the collapsed phase in  $\text{CaFe}_2\text{As}_2$  starts when the  $\text{FeAs}_4$  tetrahedral volume (at 300 K as well as at 40 K) reaches a value of about  $20.5 \text{ \AA}^3$ . It is clear from Fig. 10 that in the collapsed phase, the  $\text{FeAs}_4$  tetrahedra are much less compressible at 40 K than at 300 K. This is also consistent with the pressure variation of the As-Fe-As bond angle and Fe-As bond length (Fig. 13) in  $\text{CaFe}_2\text{As}_2$  at 300 and 40 K. We recall, as shown earlier, that the transition to the collapsed phase in  $\text{BaFe}_2\text{As}_2$  starts as the  $\text{FeAs}_4$  tetrahedral volume approaches about  $17.5 \text{ \AA}^3$ . We find significantly different pressure dependences of the polyhedral volume for the two temperatures (300 and 40 K) above 12 GPa. Since the transformation pressure in  $\text{BaFe}_2\text{As}_2$  is much higher than that in  $\text{CaFe}_2\text{As}_2$ , the Ba compound might show significant temperature dependence if measurements are extended up to much higher pressures in comparison to the transition pressure.

The calculated variation of volume with pressure for  $\text{CaFe}_2\text{As}_2$  using *ab initio* methods<sup>20</sup> gives bulk modulus values of 56.2 and 81.6 GPa for the tetragonal and collapsed tetragonal state, respectively. However, from our measurements, the  $B$  and  $B'$  values at 300 K in the collapsed phase (from fitting of data from 4.5 to 56 GPa) are  $74.8 \pm 1.2$  and  $4.8 \pm 0.1$  GPa, respectively, while at 40 K in the collapsed phase, these values (from fitting of data from 4 to 37.8 GPa) are found to be  $80.2 \pm 3.4$  and  $5.4 \pm 0.2$  GPa, respectively. The fitted ambient pressure volumes for the collapsed tetragonal phase at 300 and 40 K are  $170.1 \pm 0.2$  and  $167.7 \pm 0.4 \text{ \AA}^3$ , respectively. The comparison of pressure variation of  $c_t/a_t$  in both compounds ( $\text{CaFe}_2\text{As}_2$  and  $\text{BaFe}_2\text{As}_2$ ) shows (Fig. 7) that the structure of FeAs compounds becomes unstable as  $c_t/a_t$  approaches a value of 2.9, and completely transforms to the collapsed phase (Fig. 7) near the  $c_t/a_t$  value of 2.7. Furthermore, the transition to the collapsed phase in  $\text{CaFe}_2\text{As}_2$  occurs (Fig. 7) at nearly

the same volume of about  $165 \text{ \AA}^3$  upon compression as in the case of  $\text{BaFe}_2\text{As}_2$  at both 300 and 33 K.

#### IV. SUMMARY

In summary, we have carried out high-pressure powder synchrotron x-ray diffraction studies over a wide range of pressures and temperatures. Detailed analysis of the data for  $\text{BaFe}_2\text{As}_2$  at 300 K shows a phase transition from the tetragonal to the collapsed tetragonal phase at about 27 GPa that remains stable up to 56 GPa. The transition pressure is determined from the average of the inflection points of the hysteresis loop. On the other hand, while increasing the pressure at 33 K, we observe an onset of a transformation from an orthorhombic to a tetragonal phase at 29 GPa. Measurements on  $\text{CaFe}_2\text{As}_2$  confirm the transition to the collapsed phase as reported in the literature. We have not found any evidence of a post-collapsed tetragonal phase transition in  $\text{CaFe}_2\text{As}_2$  up to 51 GPa (at 300 K) and 37.8 GPa (at 40 K). The transition to a collapsed phase occurs in the two compounds at nearly the same values of unit-cell volume and  $c_t/a_t$  ratio. High-pressure resistivity measurements in  $\text{EuFe}_2\text{As}_2$  (Ref. 16) indicate a possible enhancement of  $T_c$  from 22 to 41 K at the transition to the collapsed phase. It would be interesting to search for superconductivity in the high-pressure phase of  $\text{BaFe}_2\text{As}_2$ .

#### ACKNOWLEDGMENTS

R.M. and S.K.M. thank the Department of Science and Technology (DST), India for providing financial support to carry out synchrotron x-ray diffraction at European Synchrotron Radiation Facility, Grenoble, France. We thank M. Hanfland and W. Crichton for loading the helium into the cells for our measurements carried out at ESRF.

- <sup>1</sup>Y. Kamihara, T. Watanabe, M. Hirano, and H. Hosono, *J. Am. Chem. Soc.* **130**, 3296 (2008).
- <sup>2</sup>M. Rotter, M. Tegel, and D. Johrendt, *Phys. Rev. Lett.* **101**, 107006 (2008).
- <sup>3</sup>P. L. Alireza, Y. T. C. Ko, J. Gillett, C. M. Petrone, J. M. Cole, G. G. Lonzarich, and S. E. Sebastian, *J. Phys. Condens. Matter* **21**, 012208 (2009).
- <sup>4</sup>W. Yu, A. A. Aczel, T. J. Williams, S. L. Bud'ko, N. Ni, P. C. Canfield, and G. M. Luke, *Phys. Rev. B* **79**, 020511(R) (2009).
- <sup>5</sup>Y. Su, P. Link, A. Schneidewind, Th. Wolf, P. Adelman, Y. Xiao, M. Meven, R. Mittal, M. Rotter, D. Johrendt, Th. Brueckel, and M. Loewenhaupt, *Phys. Rev. B* **79**, 064504 (2009).
- <sup>6</sup>Y. Xiao, Y. Su, R. Mittal, T. Chatterji, T. Hansen, C. M. N. Kumar, S. Matsuishi, H. Hosono, and Th. Brueckel, *Phys. Rev. B* **79**, 060504(R) (2009).
- <sup>7</sup>A. I. Goldman, D. N. Argyriou, B. Ouladdiaf, T. Chatterji, A. Kreyssig, S. Nandi, N. Ni, S. L. Bud'ko, P. C. Canfield, and R. J. McQueeney, *Phys. Rev. B* **78**, 100506(R) (2008).
- <sup>8</sup>R. Mittal, Y. Su, S. Rols, T. Chatterji, S. L. Chaplot, H. Schober, M. Rotter, D. Johrendt, and Th. Brueckel, *Phys. Rev. B* **78**, 104514 (2008).
- <sup>9</sup>R. Mittal, Y. Su, S. Rols, M. Tegel, S. L. Chaplot, H. Schober, T. Chatterji, D. Johrendt, and Th. Brueckel, *Phys. Rev. B* **78**, 224518 (2008).
- <sup>10</sup>R. Mittal, L. Pintschovius, D. Lamago, R. Heid, K. -P. Bohnen, D. Reznik, S. L. Chaplot, Y. Su, N. Kumar, S. K. Dhar, A. Thamizhavel, and Th. Brueckel, *Phys. Rev. Lett.* **102**, 217001 (2009).
- <sup>11</sup>R. Mittal, R. Heid, A. Bosak, T. R. Forrest, S. L. Chaplot, D. Lamago, D. Reznik, K.-P. Bohnen, Y. Su, N. Kumar, S. K. Dhar, A. Thamizhavel, Ch. Rüegg, M. Krisch, D. F. McMorrow, Th. Brueckel, and L. Pintschovius, *Phys. Rev. B* **81**, 144502 (2010).
- <sup>12</sup>A. Kreyssig, M. A. Green, Y. Lee, G. D. Samolyuk, P. Zajdel, J. W. Lynn, S. L. Bud'ko, M. S. Torikachvili, N. Ni, S. Nandi, J. B. Leao, S. J. Poulton, D. N. Argyriou, B. N. Harmon, R. J. McQueeney, P. C. Canfield, and A. I. Goldman, *Phys. Rev. B* **78**, 184517 (2008).
- <sup>13</sup>A. I. Goldman, A. Kreyssig, K. Prokes, D. K. Pratt, D. N. Argyriou, J. W. Lynn, S. Nandi, S. A. J. Kimber, Y. Chen, Y. B. Lee, G. Samolyuk, J. B. Leao, S. J. Poulton, S. L. Bud'ko, N. Ni, P. C. Canfield, B. N. Harmon, and R. J. McQueeney, *Phys. Rev. B* **79**, 024513 (2009).
- <sup>14</sup>S. A. J. Kimber, A. Kreyssig, Yu-Zhong Zhang, H. O. Jeschke, R. Valentí, F. Yokaichiya, E. Colombier, J. Yan, T. C. Hansen, T. Chatterji, R. J. McQueeney, P. C. Canfield, A. I. Goldman, and D. N. Argyriou, *Nat. Mater.* **8**, 471 (2009).
- <sup>15</sup>J.-E. Jørgensen, J. Staun Olsen, and L. Gerward, *Solid State Commun.* **149**, 1161 (2009).
- <sup>16</sup>W. Uhoja, G. Tsoi, Y. K. Vohra, M. A. McGuire, A. S. Sefat, B. C. Sales, D. Mandrus, and S. T. Weir, *J. Phys. Condens. Matter* **22**, 292202 (2010).
- <sup>17</sup>Yu-Z. Zhang, I. Opahle, H. O. Jeschke, and R. Valentí, *J. Phys. Condens. Matter* **22**, 164208 (2010).
- <sup>18</sup>G. Garbarino, P. Toulemonde, M. Alvarez-Murga, A. Sow, M. Mezouar, and M. Nunez-Regueiro, *Phys. Rev. B* **78**, 100507(R) (2008).
- <sup>19</sup>G. Garbarino, A. Sow, P. Lejay, A. Sulpice, P. Toulemonde, M. Mezouar, and M. Nunez-Regueiro, *Europhys. Lett.* **86**, 27001 (2009).
- <sup>20</sup>T. Yildirim, *Phys. Rev. Lett.* **102**, 037003 (2009).
- <sup>21</sup>T. Yamazaki, N. Takeshita, R. Kobayashi, H. Fukazawa, Y. Kohori, K. Kihou, C.-H. Lee, H. Kito, A. Iyo, and H. Eisaki, *Phys. Rev. B* **81**, 224511 (2010).
- <sup>22</sup>W. J. Duncan, O. P. Welzel, C. Harrison, X. F. Wang, X. H. Chen, F. M. Grosche, and P. G. Niklowitz, *J. Phys. Condens. Matter* **22**, 052201 (2010).
- <sup>23</sup>S. O. Diallo, D. K. Pratt, R. M. Fernandes, W. Tian, J. L. Zarestky, M. Lumsden, T. G. Perring, C. L. Broholm, N. Ni, S. L. Bud'ko, P. C. Canfield, H.-F. Li, D. Vaknin, A. Kreyssig, A. I. Goldman, and R. J. McQueeney, *Phys. Rev. B* **81**, 214407 (2010).
- <sup>24</sup>Y. Xiao, Y. Su, R. Mittal, T. Chatterji, T. Hansen, S. Price, C. M. N. Kumar, J. Persson, S. Matsuishi, Y. Inoue, H. Hosono, and Th. Brueckel, *Phys. Rev. B* **81**, 094523 (2010).
- <sup>25</sup>D. Kasinathan, A. Ormeci, K. Koch, U. Burkhardt, W. Schnelle, A. L. Jasper, and H. Rosner, *New J. Phys.* **11**, 025023 (2009).
- <sup>26</sup>Y. Z. Zhang, H. C. Kandpal, I. Opahle, H. O. Jeschke, and R. Valentí, *Phys. Rev. B* **80**, 094530 (2009).
- <sup>27</sup>Y. Wang, Y. Ding, and J. Ni, *Solid State Commun.* **149**, 2125 (2009).
- <sup>28</sup>A. S. Sefat, R. Jin, M. A. McGuire, B. C. Sales, D. J. Singh, and D. Mandrus, *Phys. Rev. Lett.* **101**, 117004 (2008).
- <sup>29</sup>M. D. Lumsden, A. D. Christianson, D. Parshall, M. B. Stone, S. E. Nagler, G. J. MacDougall, H. A. Mook, K. Lokshin, T. Egami, D. L. Abernathy, E. A. Goremychkin, R. Osborn, M. A. McGuire, A. S. Sefat, R. Jin, B. C. Sales, and D. Mandrus, *Phys. Rev. Lett.* **102**, 107005 (2009).
- <sup>30</sup>M. S. Torikachvili, S. L. Bud'ko, N. Ni, and P. C. Canfield, *Phys. Rev. Lett.* **101**, 057006 (2008).
- <sup>31</sup>M. S. Torikachvili, S. L. Bud'ko, N. Ni, P. C. Canfield, and S. T. Hannahs, *Phys. Rev. B* **80**, 014521 (2009).
- <sup>32</sup>M. Rotter, M. Tegel, D. Johrendt, I. Schellenberg, W. Hermes, and R. Pöttgen, *Phys. Rev. B* **78**, 020503(R) (2008).
- <sup>33</sup>T. Park, E. Park, H. Lee, T. Klimczuk, E. D. Bauer, F. Ronning, and J. D. Thompson, *J. Phys. Condens. Matter* **20**, 322204 (2008).
- <sup>34</sup>K. Prokes, A. Kreyssig, B. Ouladdiaf, D. K. Pratt, N. Ni, S. L. Bud'ko, P. C. Canfield, R. J. McQueeney, D. N. Argyriou, and A. I. Goldman, *Phys. Rev. B* **81**, 180506(R) (2010).
- <sup>35</sup>H. Takahashi, K. Igawa, K. Arii, Y. Kamihara, M. Hirano, and H. Hosono, *Nature (London)* **453**, 376 (2008).
- <sup>36</sup>B. Lorenz, K. Sasmal, R. P. Chaudhury, X. H. Chen, R. H. Liu, T. Wu, and C. W. Chu, *Phys. Rev. B* **78**, 012505 (2008).
- <sup>37</sup>S. Margadonna, Y. Takabayashi, Y. Ohishi, Y. Mizuguchi, Y. Takano, T. Kagayama, T. Nakagawa, M. Takata, and K. Prassides, *Phys. Rev. B* **80**, 064506 (2009).
- <sup>38</sup>N. Tateiwa and Y. Hag, *Rev. Sci. Instrum.* **80**, 123901 (2009).
- <sup>39</sup>A. P. Hammersley, Report No. EXP/AH/95-01 (1995).
- <sup>40</sup>J. Rodriguez-Carvajal, *Physica B* **192**, 55 (1992).